www.czasopisma.pan.pl PAN www.journals.pan.pl
POLSKA AKADEMIA NAUK
jet INTL JOURNAL OF ELECTRONICS AND TELECOMMUNICATIONS, 2021, VOL. 67, NO. 3, PP. 409-416
Manuscript received January 13, 2021; revised July, 2021 DOI: 10.24425/ijet.2021.137827

Investigation of Different Transfer Functions for Optical Limiting Amplifier used in a 2R Burst Mode Optical Regenerator

Yash Deodhar, Jeeru Jaya Sankar Reddy, Priyanka Desai Kakade, and Rohan Kakade

***Abstract*—the major difference between a continuous mode optical regenerator (CMOR) and a burst mode optical regenerator (BMOR) is that a BMOR is capable of handling large variations in the input power which makes it useful in optical packet switched and optical burst switched networks. This is due to the optical limiting amplifier (OLA) present in the BMOR. Using computer modelling, the impact of using different OLA non-linear transfer functions on the output bit error rate of a system consisting of a cascade of 2R BMORs has been investigated. The effect of amplified spontaneous emission (ASE) noise introduced in the inter-regenerator links has also been taken into consideration. Also, a brief review of existing OLA designs is presented.**

***Keywords*—optical limiting amplifier, burst mode, ASE noise, nonlinearity, bit error rate, optical regeneration**

I. Introduction

In all optical networks (AONs), the degradation caused by various optical impairments is eliminated or minimised by using an optical regenerator (OR). An OR attempts to restore the quality of an impaired signal to that of the originally transmitted signal by reamplifying (1R), reshaping (2R) and retiming (3R) the impaired signal [1]–[3]. 1R ORs are those that only attempt reamplification of the impaired signals and are commonly known as optical amplifiers (OAs). ORs that reamplify and reshape the impaired signal are called 2R ORs while ORs that provide all the signal restoration functionalities are called 3R ORs. Optical networks that deal with a continuous stream of data use continuous mode optical regenerators (CMORs) [4]. As these CMOR based optical networks have inherently low bandwidth efficiency and flexibility, optical packet switched (OPS) and optical burst switched (OBS) network topologies serve as promising alternatives [5]. OPS/OBS networks are capable of handling optical packets/bursts of data, which arrive at an optical node from various transmitters. Due to the presence of multiple transmitters and potential for each of their packet/burst transmissions to traverse varying optical path lengths to reach a given node, each data packet transmitted suffers differential amounts of attenuation. Thus, optical packets/bursts with a wide range of power levels are received at the input of an OR at an optical node. Due to the limited input power range of the CMOR, it fails to adapt to the varying input power levels of the incoming optical packets/bursts in OPS/OBS network topologies [6], [7]. A different type of OR, which can adapt its response based on the received signal power level, called a burst mode optical regenerator (BMOR), is thus used in such networks.

Various models have been proposed for a BMOR. In the 2R BMOR model (see Fig. 1) proposed by Sato *et al.* [8], a gain-saturated semiconductor optical amplifier (GS-SOA) with an assisted signal is the optical limiting amplifier (OLA) used to provide the power equalization required for the packet-to-packet power variations in burst mode systems. The GS-SOA is followed by a monolithic integrated wavelength converter, which acts as a non-linear reshaper. Within the OLA, the incoming packets are divided by the optical coupler into two parts so as to allow directing some packets to pass through an optical filter and the rest to pass through another SOA which acts as a cross-gain modulation (XGM) based wavelength converter. In the model, then a continuous wave (CW) light signal was passed into the XGM-SOA to create an inverted mode signal. This was then passed through the same optical coupler and through an optical circulator was input to the GS-SOA. So, the original and inverted mode signals were input to the GS-SOA together and with assistance of the inverted mode signal in the suppression of the pattern effects, the total average input power into the GS-SOA was maintained almost constant. Thus, the output signal had a limited power.

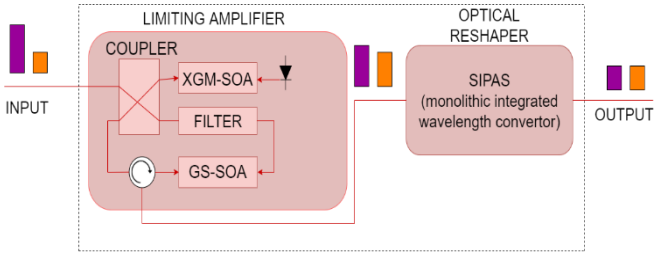

Fig. 1. Block diagram of all-optical 2R BMOR (redrawn from [8])

In the 3R BMOR model proposed by Kanellos *et al.* [9] four cascaded hybrid integrated SOA–Mach–Zehnder interferometer (MZI) switches have been used. Here, the 2R optical regeneration is performed entirely by the first SOA-MZI which exploits the SOA gain dynamics to effectively handle the

Yash Deodhar, Jeeru Jaya Sankar Reddy are with Manipal Institute of Technology, Manipal Academy of Higher Education (e-mail: yashd1618@gmail.com, jayasankarreddy0@gmail.com).

Priyanka Desai Kakade (corresponding author) is with Department of Electronics And Communication Engineering, Manipal Institute of Technology, Manipal Academy of Higher Education, Manipal, Karnataka, India-576104, (e-mail: priyanka.kakade@manipal.edu).

Rohan Kakade (Corresponding Author) is with Loughborough University, United Kingdom, (e-mail: R.N.Kakade@lboro.ac.uk).

incoming packet power variations. The couplers, with their unbalanced splitting ratio, provide the necessary nonlinear reshaping transfer function required. Zakynthios *et al.* [10] present another model where a single MZI switch is used in a loop configuration to demonstrate the cascaded operation of a 2R BMOR in an OBS network. Here the power variations of the packets were managed by using a loop configuration with a modulator placed within it. The modulator provides attenuation to a part of the data, as it repeatedly circulates in the loop, before the data enters the BMOR. Another 3R BMOR is demonstrated in the work by Petrantonakis *et al.* [11] using 3 hybrid integrated quad SOA-MZI arrays. Either power equalisation, clock recovery or data regeneration was performed by one of these 3 quad HZMIs. The first quad HMZI provides the power equalisation, thus acting as the optical limiting amplifier (OLA); it deals with the power variations of the packets by exploiting the unequal splitting ratios and using different current values for their two SOAs. Thus, providing higher gain to low power packets and lower gain to high power packets. All aforementioned papers [8]–[11] thus present a unique model of a BMOR, but as mentioned in [6], each of these models can be interpreted as an optical limiting amplifier (OLA) followed by a non-linear optical reshaper.

In OBS/OPS networks, the OLA is what makes BMORs more applicable than CMORs in handling unequal packet power levels by providing power equalization [6], [12]. As seen in the models mentioned above [8]–[11], in burst mode applications, most OLAs are built using SOA technology. In Desai *et al.* [6], the transfer function (TF) of the OLA has been approximated to be a linear function to help simplify the complex model of a BMOR. However, it should be noted that practically the TF of the OLA might not be linear. Table 1 shows the summary of OLA designs used in various applications. In this paper, for the first time, a numerical model of a cascade of 10 BMORs, incorporating a non-linear TF for OLA has been investigated. Different non-linear TFs for OLA are modelled (explained in section 2) and a system performance comparison is presented between these non-linear TFs and with the linear TF for OLA described in [6]. In all the cases that are analysed, the same non-linear reshaping element has been considered to provide a consistent comparison of the different TFs for an OLA. Further, the effect of amplified spontaneous noise (ASE) noise on the optical signal has also been incorporated into the model.

The rest of this paper is organised as follows. Section 2 provides the numerical model of the BMOR cascade and the different OLA TFs that have been chosen for investigation. Section 3 discusses the results obtained and Section 4 presents the conclusion.

TABLE I
SUMMARY OF OLA DESIGNS

Technology	Description
SOA	• Gain saturated SOA with XGM wavelength convertor [6] • 3R BMOR using Mach–Zehnder interferometer (MZI) switch cascade [7] • Single MZI switch in loop configuration to model a 2R BMOR [8] • 3 hybrid integrated quad SOA-MZI arrays acting as a 3R BMOR [9] • Power equalisation using a SOA-XGM followed by an MZI [13] • All-optical packet equalizer based on non-linear polarization rotation (NPR) in a SOA [14] • All-optical power equalization using a SOA as a gain stage followed by an SOA operating in saturation region [15] • Interferometric gate based on SOA used as optical power limiter [16] • SOA used as OLA and power booster for a single channel RZ-DPSK signal [17] • SOA acting as optical limiting amplifier in Next Generation Passive Optical Networks (NG-PON) [18] • Multi-wavelength all-optical regeneration based on inhomogenously broadened gain of self-assembled quantum dots in quantum dot SOAs. [19] • Increasing dynamic range of DPSK packet receivers using fast optical limiting amplifiers consisting of SOAs [20]
EDFA	• Differential lump-loss incorporation within EDFA [21] • Two stage amplifier with an isolator and synchronized etalon filter [22] • Inserting a bidirectional between an optical circulator and a Fiber Bragg Grating (FBG) [23] • Chirp-fiber-grating based erbium doped optical amplifier [24] • Multi-wavelength wavelength-division-multiplexing (WDM) OLA using 2 stage EDFA [25] • WDM bidirectional power limiting amplifier using circulators, fiber grating and EDFA [26]
Other fiber based amplifiers	• 2 section gain flattened fiber parametric amplifier used for power equalisation [27] • Optical limiter based on self-phase modulation (SPM) and made of highly non-linear fiber (HNLF) and dispersion compensating fibers (DCF) [28]

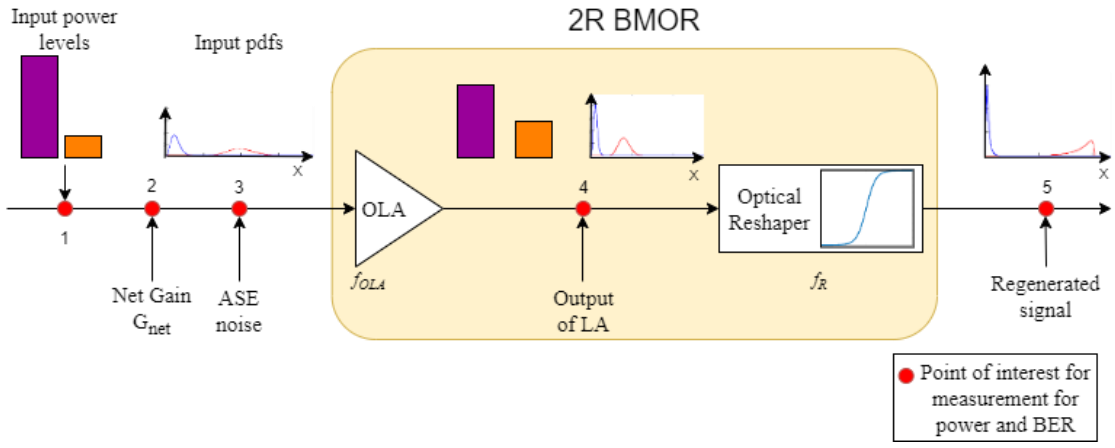

Fig 2. Model of a 2R BMOR

II. Numerical Model of 2R BMOR Cascade with a Non-Linear OLA

Figure 2 is a graphical representation of a single 2R BMOR in the BMOR cascade. In this paper, the power level corresponding to the bit '1' has been assigned to the maximum power that goes unchanged through the optical reshaper. This holds true for all cases where different OLA TFs are used as the same reshaping element has been used in every case.

The OLA achieves power equalization by providing higher gain to soft (lower power) packets and lower gain to hard (high power) packets. Its normalized TF is given by [6]:

$$y_{avg} = f_{OLA}(x_{avg}) \tag{2}$$

where x_{avg} is the normalized average input power to the OLA and y_{avg} is the normalized output power of the OLA. This function also decides the gain (G_{LA}) provided by the OLA. G_{LA} is defined as $G_{LA} = y_{avg}/x_{avg} = f_{OLA}(x_{avg})/x_{avg}$.

For every TF investigated for OLA in this work, a target operating point (x_{tar}, y_{tar}) has been fixed where y_{tar} is the target output power of the OLA for a specific input power x_{tar}. All the OLA TFs discussed in this paper have been selected to have the same y_{tar} and x_{tar} to maintain a consistent comparison between them.

The normalized equation of the linear OLA TF used in Desai *et al* [6], [7] has been used here. The three non-linear OLA TFs that have been chosen for the analysis are the exponential function, the logarithmic function and the piecewise function (that exhibits an exponential and a logarithmic behaviour depending on the input power level). These have been defined as,

$$f_{lin}(x) = (m_1 \cdot x) + h_1 \tag{2}$$

$$f_{exp}(x) = (m_2 \cdot e^x) + h_2 \tag{3}$$

$$f_{log}(x) = (m_3 \cdot \ln(x)) + h_3 \tag{4}$$

$$f_{piecewise}(x) = \begin{cases} (m_4 \cdot e^x) + h_4, & 0 \le x < x_{tar} \\ (m_5 \cdot \ln(x)) + h_5, & x_{tar} \le x < \infty \end{cases} \tag{5}$$

where each pair of (m, h) determines the gain (G_{LA}) provided by the OLA for their corresponding TF.

The optical reshaper used in a BMOR being conceptually the same as that used in a CMOR they can be characterised by same TFs. The hyperbolic tangent function employed in Desai *et al* [6] to describe the optical reshaper TF there for CMOR use has been employed in this work.

$$f_{RTF}(x) = a_1 \cdot \tanh\left(a_2 \cdot \left(x - \frac{1}{2}\right)\right) + a_3 \tag{6}$$

a_1, a_2 and a_3 are evaluated using $f_{RTF}(0) = 10^{-r_{NL}/10}$, $f_{RTF}(1) = 1$ and $df_{RTF}(x)/dx\,|_{x=d_{RG}} = 1/\gamma$ where r_{NL} is non-linear extinction, d_{RG} is the nonlinear threshold (here assumed to be equal to $1/2$) and γ value lies between 0 and 1, is the non-linearity degree related to the optical reshaper (lower γ implies that reshaper is more non-linear) [6], [29].

Because of ASE noise, the 1's and 0's of the input packets to the BMOR are represented by probability density functions (pdfs). The pdf distributions are non-central chi-square (NCCS) distributions with four degrees of freedom [6], [23], [29] and are defined as follows:

$$pdf_j(x) = \frac{1}{2\sigma^2}\left(\frac{x}{P_j}\right)^{\frac{M-1}{2}} e^{-\left(\frac{x+P_j}{2\sigma^2}\right)} I_{M-1}\left(\frac{\sqrt{xP_j}}{\sigma^2}\right) \tag{7}$$

where $j = 1$ indicates pdf of/ power in data = 1, $j = 0$ indicates pdf of/power in data = 0 and M equals B_{opt}/B where B_{opt} is the optical bandwidth and B is the bit rate and σ^2 is the variance for each of the Gaussian random variables related to ASE noise components in each of the quadratures and polarisations. [6], [29]

Furthermore, pdf_{j1} at the output of i^{th} BMOR i.e. at point 1, is affected by the net gain G_i that arises due to the fibre section leading up to the input of $(i+1)^{th}$ BMOR. The new pdf can be described by,

$$pdf_{j2}(x) = \left|\frac{1}{G_i}\right| pdf_{j1}(x \cdot G_i) \tag{8}$$

which can be deduced by using the pdf transformation rule given as [30]:

$$pdf_Y(y) = \left|\frac{dx}{dy}\right| pdf_X(x), \quad (9)$$

where X and Y are the input and output random variables respectively.

This pdf in turn also gets affected by ASE noise and thus gets modified as follows [6]:

$$pdf_{j3}(y) = \int_0^\infty pdf_{ASE}(y|x) \cdot pdf_{j2}(x)\, dx \quad (10)$$

where,

$$pdf_{ASE}(y|x) = \frac{1}{2\sigma_i^2}\left(\frac{y}{x}\right)^{\frac{M-1}{2}} e^{-\left(\frac{y+x}{2\sigma_i^2}\right)} \mathrm{I}_{M-1}\left(\frac{\sqrt{y \cdot x}}{\sigma_i^2}\right) \quad (11)$$

and $\sigma_i{}^2$ is related to the ASE noise contributed by the cascade of amplifier between the i^{th} and $(i+1)^{\text{th}}$ BMORs. The pdf given in equation (9) is the final input to the OLA of the next BMOR. Once a packet passes through the OLA, its pdfs are affected by the gain of the OLA at the $i+1^{\text{th}}$ BMOR ($G_{OLA_{i+1}}$) and hence the pdfs at the output of the OLA are:

$$pdf_{j4}(y) = \left|\frac{1}{G_{OLA_{i+1}}}\right| pdf_{j3}\left(y \cdot G_{OLA_{i+1}}\right) \quad (12)$$

These pdfs then enter the optical reshaper to be re-transformed (as modelled by the by equation (5)). Thus, the pdf at the output of the optical reshaper (and BMOR) is given by:

$$pdf_{j5}(z) = \left|\frac{dy}{dz}\right| pdf_{j4}(y) \quad (13)$$

where $\frac{dy}{dz} = \frac{1}{ab}\cosh^2\left((y - \frac{1}{2}) \cdot b\right)$ for $y \leq k$ and $\frac{dy}{dz} = \frac{1}{ab}\cosh^2\left((k - \frac{1}{2}) \cdot b\right)$ for $y > k$.

Finally, to compare the different OLA TF's, the BER is calculated at a given point in the cascade of BMORs using the following formula:

$$BER_n = \int_0^{p_{th\_n}} pdf_{1n}(x)dx + \int_{p_{th\_n}}^\infty pdf_{0n}(x)dx, \quad (14)$$

where p_{th_n} is the optimum decision threshold obtained by calculating $pdf_{0n}(p_{th\_n}) = pdf_{1n}(p_{th\_n})$ and n indicates the point of interest in the model to determine BER .

III. Results and Discussion

In this paper, the transmitter output signal and the output signal from each BMOR is assumed to have a 50% return-to-zero (RZ) format. Due to this, the average output packet power from every BMOR is calculated as follows: $P_{\text{av}} = \frac{P_1+3P_0}{4} = 0.25$, where $P_1 = 1$ and $P_0 = 0$. Moreover, x_{tar} has been assigned the value $x_{tar} = 0.25 \cdot G_{\text{netnom}}$ where G_{netnom} is the nominal (target) value of G_{net} which is assumed to be 5dB as also used in [6]. Furthermore, in-line with what is implemented in [6], the value of y_{tar} is assumed to be 0.4 as there is a trade-off between the low and high power requirements.

A. Output average power vs input average power characteristics for different OLA TFs

For every OLA TF, different m values are investigated to observe the output power for a range of input powers and the results are presented in Fig. 3.

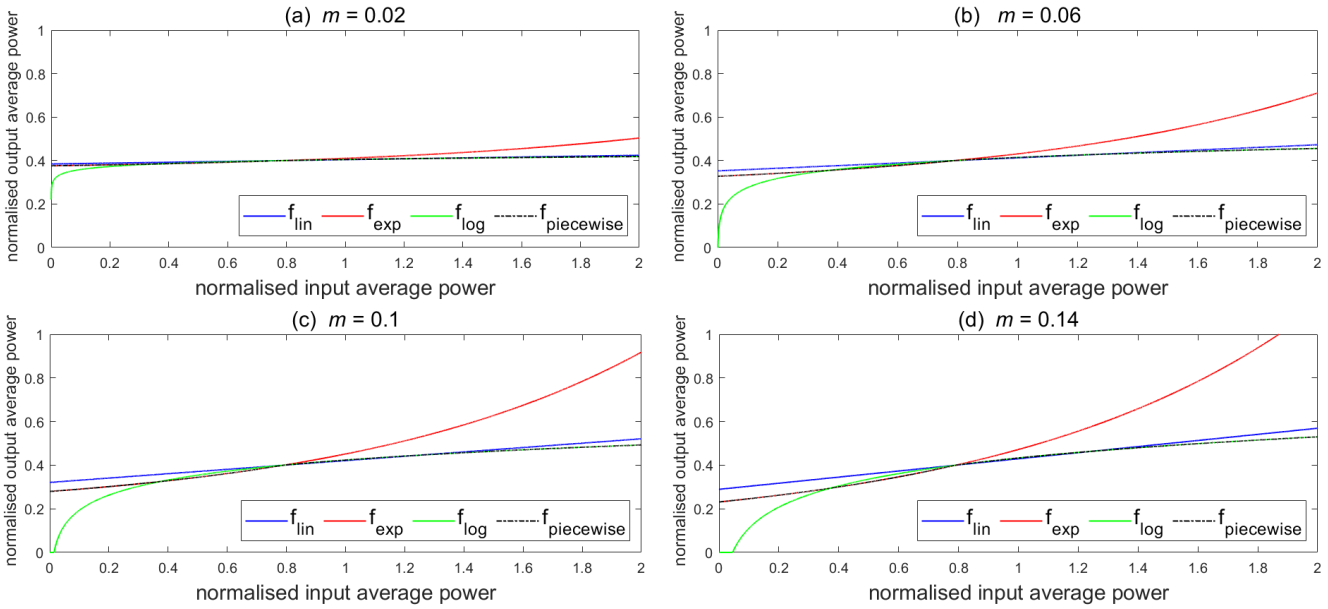

Fig. 3. Output Average Power as a function of input average power for the different OLA TFs with $m_1 = m_2 = m_3 = m_4 = m_5 = m$ with (a) $m = 0.02$, (b) $m = 0.06$, (c) $m = 0.1$, and (d) $m = 0.14$

As discussed at the start of the section, for any input average power the OLA TF should give an output average power of 0.4. It can be seen in Fig. 3, for higher values of m, the logarithmic and exponential TFs are not able to provide the target output power of 0.4 for lower and higher input powers respectively but for $m = 0.02$ all four OLA TFs are able to perform power equalization effectively.

It can also be seen that the linear TF f_{lin} is a good approximation of the exponential TF for low input average powers while it is a good approximation of logarithmic TF for higher input powers. It can also be observed that the piecewise TF provides the same output average power as the exponential TF for input values less than x_{tar} and the same output power as the logarithmic TF for input power values greater than x_{tar}.

It can be observed that the threshold required will be closer to the 0's than 1's owing to the noisier incoming packets of 1's compared to that of the 0's (considering the OR's effective power detection). As the threshold varies depending on the input average packet power, we can thus say that m cannot be equal to 0 and choice of any value will be a compromise. [6].

B. BER at the cascade output vs m

Different values of γ were examined to see its impact on the BMOR cascade and its effect on the output BER of the 10th BMOR. The results were obtained for input average packet power $P_{\text{avin}} = 0.25$ (soft packet) and $P_{\text{avin}} = 1$ (hard packet) and the slopes of the OLA TFs were varied to make a fair comparison of the different OLA TFs. From Fig. 4 it can clearly be seen that for $P_{\text{avin}} = 1$, for both values of γ, the linear TF gives the best BER. It should be noted, that the very low BER values in Fig. 4(b) cannot be realized practically but aid in understanding the impact of the various parameters.

As seen in Fig. 5 for $P_{\text{avin}} = 0.25$ and $\gamma = 0.5$ the logarithmic TF provides the lowest BER. For $P_{\text{avin}} = 0.25$ be noted that for $\gamma = 0.2$, the output BER is generally much lower than when $\gamma = 0.5$, keeping all other factors constant. Hence, it can be concluded that a lower γ will give lower and $\gamma = 0.2$, it is observed that logarithmic TF provides the lowest BER when the $m = 0.02$ and the exponential TF provides the lowest BER when $m = 0.06$. However, for $m > 0.1$, the linear TF provides the lowest BER. It should output BER irrespective of m for $P_{\text{avin}} = 1$, but in case of $P_{\text{avin}} = 0.25$ higher m values give worse BER for $\gamma = 0.2$ as compared to $\gamma = 0.5$.

C. BER evolution along the cascade of 2R BMORs

The effect of P_{avin} (input average power to 1st BMOR) on the BER at the output of each BMOR in the cascade has been investigated in order to determine which OLA TF is able to provide minimum BER for a wide range of input power levels. The BER was evaluated for 2 power levels, $P_{\text{avin}} = 0.25$ and $P_{\text{avin}} = 1$ and each case has further been studied for $\gamma = 0.2$ and $\gamma = 0.5$. The OLA TFs were chosen to be such that $m_1 = m_2 = m_3 = m_4 = m_5 = m$. $m = 0.02$ and $m = 0.14$ were investigated to acquire results for a wide range of values of m. It can be seen from Fig. 6 that for $P_{\text{avin}} = 1$, for both values of γ the linear TF and logarithmic TF provide the almost the same BER which is much lower than the BER provided by the exponential TF, with the linear TF performing slightly better than the logarithmic TF for $m = 0.14$. Furthermore, it can be seen in Fig. 7 that for $P_{\text{avin}} = 0.25$, the linear TF provides the lowest BER for $m = 0.14$ while logarithmic provides the lowest BER for $m = 0.02$. Thus, both logarithmic and linear OLA TFs are capable of dealing with a wide range of power, with linear TF performing better at $m = 0.14$ and logarithmic performing slightly better at $m = 0.02$.

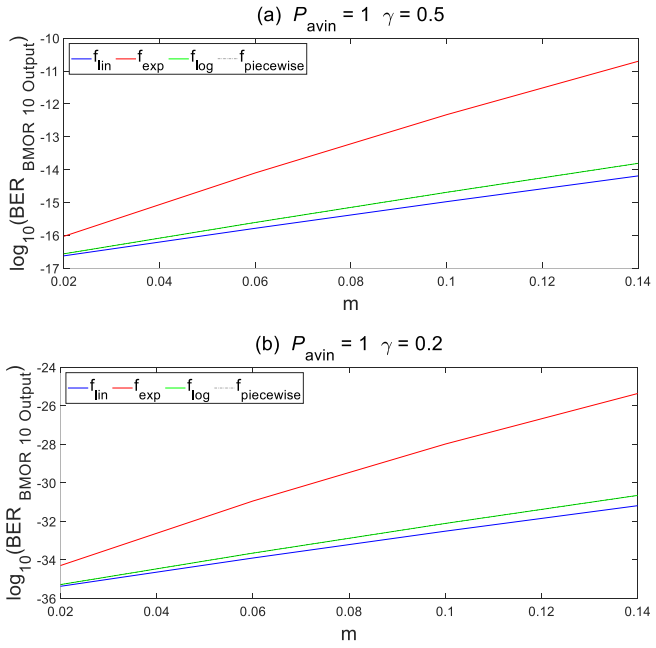

Fig. 4. Output BER of the 10th BMOR in the cascade for different values of m with (a) $P_{\text{avin}} = 1$ and $\gamma = 0.5$, (b) $P_{\text{avin}} = 1$ and $\gamma = 0.2$

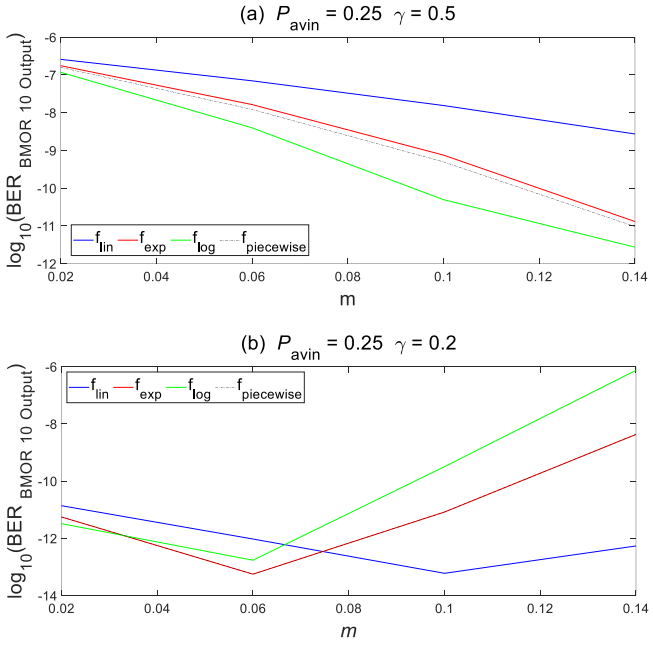

Fig. 5. Output BER of the 10th BMOR in the cascade for different values of m with (a) $P_{\text{avin}} = 0.25$ and $\gamma = 0.5$, (b) $P_{\text{avin}} = 0.25$ and $\gamma = 0.2$

D. Power Equalization performed by different OLA TFs

As stated at the start of section III, the output power of every OLA TF is set to be $y_{tar} = 0.4$. The input power to the OR was observed at each BMOR to find out which OLA TF provided the best power equalization. The OLA output power was observed for 2 power levels, $P_{\text{avin}} = 0.25$ and $P_{\text{avin}} = 1$ and each case has further been studied for $\gamma = 0.2$ and $\gamma = 0.5$ with $m = 0.02$ and $m = 0.14$. In Fig. 8 and 9 we can see that in all the cases of $\gamma = 0.2$, by the 2nd OLA output, all power levels converge to 0.4 and that value remains there for the rest of the cascade. This can also be observed in the case of $P_{\text{avin}} = 0.25$ and $\gamma = 0.5$ (Fig. 9(a)) but approximately by 4th BMOR power levels converge to 0.4. However, in the case of $P_{\text{avin}} = 1$ and $\gamma = 0.5$ (Fig. 8(a)) the exponential OLA TF fails to provide an output power of 0.4 even by the 10th BMOR. Thus, it can be concluded that the linear, logarithmic and piecewise OLA TFs are better at performing power equalization than the exponential TF.

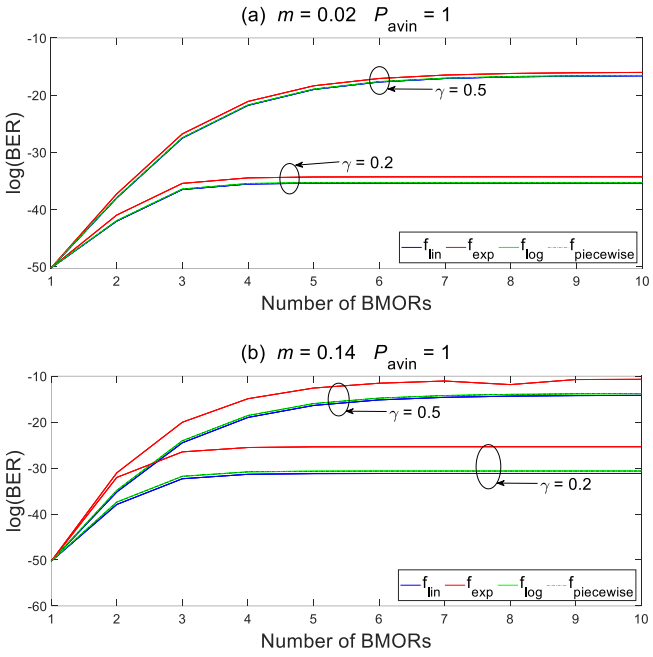

Fig. 6. Output BER evaluation along the cascade of BMORs for the different OLA TFs with (a) $m = 0.02$ and $P_{\text{avin}} = 1$, (b) $m = 0.14$ and $P_{\text{avin}} = 1$

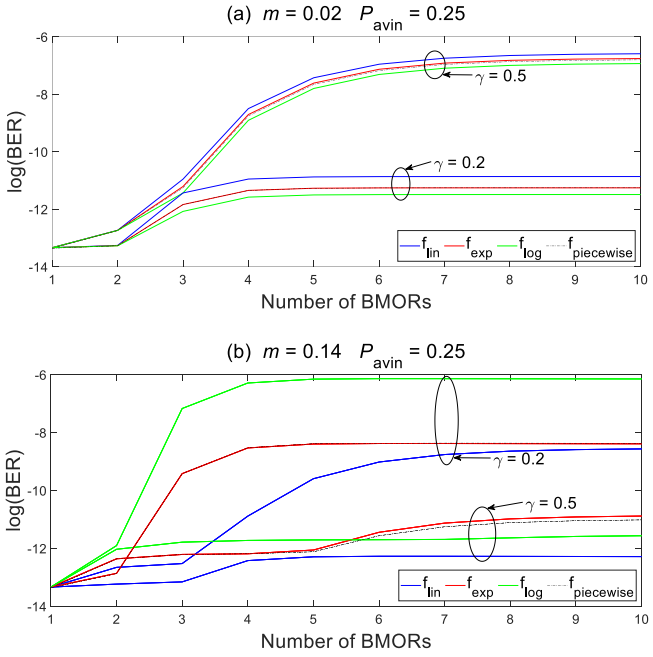

Fig. 7. Output BER evaluation along the cascade of BMORs for the different OLA TFs with (a) $m = 0.02$ and $P_{\text{avin}} = 0.25$, (b) $m = 0.14$ and $P_{\text{avin}} = 0.25$

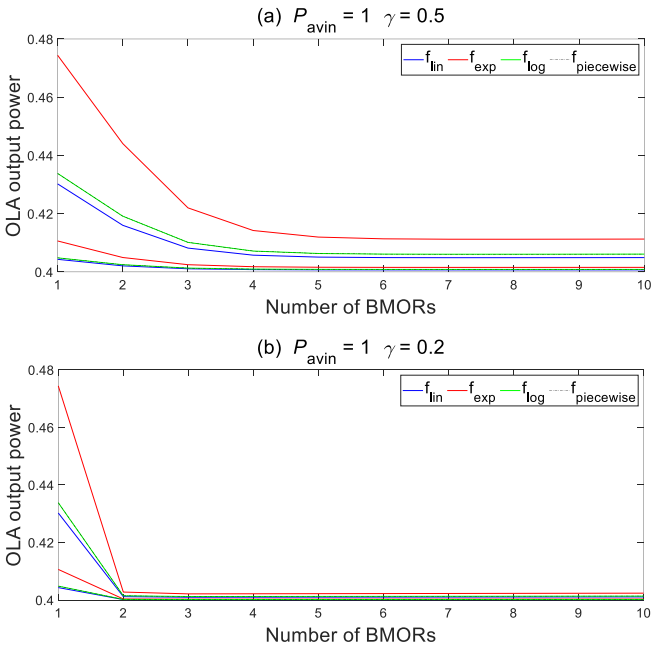

Fig 8. Output power of OLA (input power to the OR) for each BMOR along the cascade for different OLA TFs with (a) $P_{\text{avin}} = 1$, and $\gamma = 0.5$, (b) $P_{\text{avin}} = 1$ and $\gamma = 0.2$ with $m_1 = m_2 = m_3 = m_4 = m_5 = m = 0.02, 0.14$ in each case

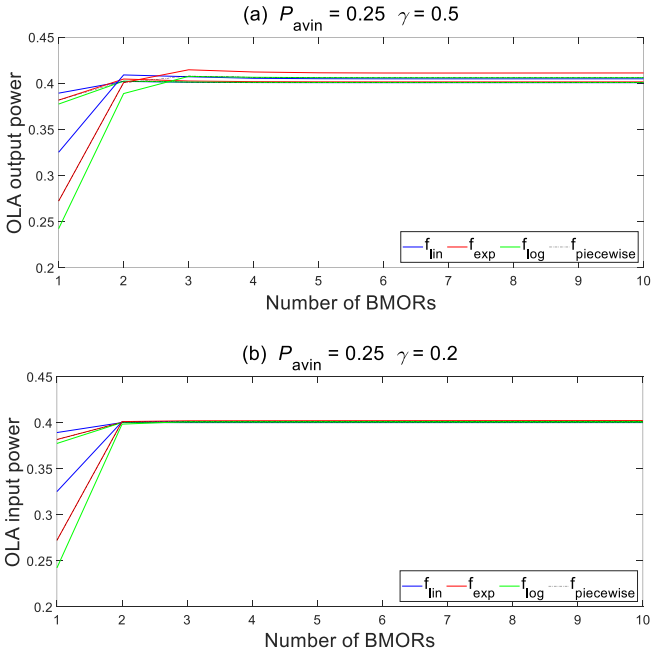

Fig 9. Output power of OLA (input power to the OR) for each BMOR along the cascade for different OLA TFs with (a) $P_{\text{avin}} = 0.25$ and $\gamma = 0.5$, (b) $P_{\text{avin}} = 0.25$ and $\gamma = 0.2$ with $m_1 = m_2 = m_3 = m_4 = m_5 = m = 0.02, 0.14$ in each case

E. BMOR output power for different OLA TFs

As discussed at the start of section III, the output power of each BMOR is calculated to be 0.25 since we have assumed the signal to be 50% RZ. The impact of different OLA TFs is observed on the output power of each BMOR for $P_{\text{avin}} = 0.25$ and $P_{\text{avin}} = 1$ with each case being studied for $\gamma = 0.2$ and $\gamma = 0.5$ with $m = 0.02$ and $m = 0.14$. It should be evident from Fig. 10 and 11 that when $\gamma = 0.2$, all cases provide similar output powers at each BMOR starting from the second BMOR. When $\gamma = 0.5$, it takes a greater number of BMORs to provide similar outputs. As seen in Fig. 10 (a), system needs 5 BMORs for the output powers to converge to 0.25 and from Fig. 11 (a), system needs 4 BMORS, for output powers to converge to 0.25. Hence, it can be concluded that if a sufficiently large number of BMORs are used in a cascade then the type of TF chosen for the OLA has less impact on the output power of the BMORs.

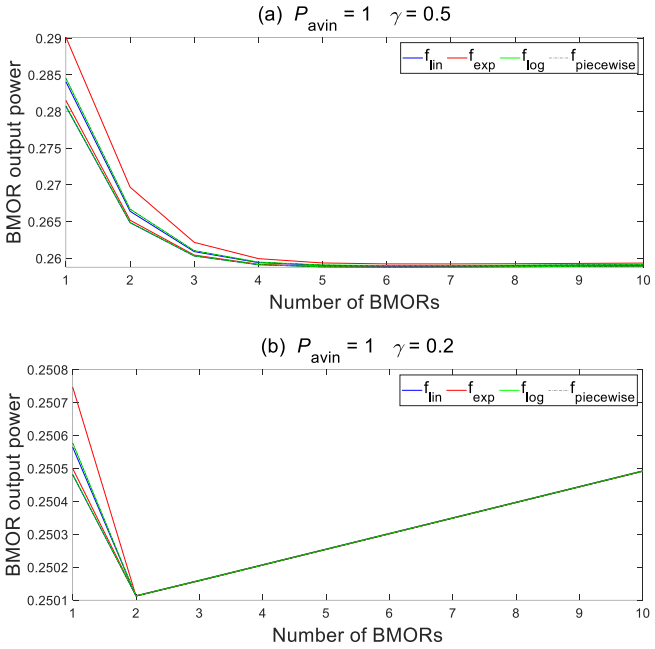

Fig. 10. Output power evaluation of each BMOR in the cascade for different OLA TFs with (a) $P_{\text{avin}} = 1$ and $\gamma = 0.5$, (b) $P_{\text{avin}} = 1$ and $\gamma = 0.2$ with $m_1 = m_2 = m_3 = m_4 = m_5 = m = 0.02, 0.14$ in each case.

IV. CONCLUSION

Different OLA TFs have been implemented in a cascade of 10 BMORs and the BER and power levels have been evaluated at various points throughout the cascade. From the numerical analysis done, it can be concluded the for $P_{\text{avin}} = 1$, a lower γ will give a lower BER irrespective of the m value used but for $P_{\text{avin}} = 0.25$ higher m values give higher BER for $\gamma = 0.2$ as compared to $\gamma = 0.5$. In addition, it was seen that from the OLA TFs chosen, the logarithmic and linear OLA TFs are the best at dealing with a wide range of power and the linear, logarithmic and piecewise OLA TFs perform better power equalisation than the exponential TF. The analysis also shows that if a cascade consists of many BMORs, the type of OLA TF chosen has less impact on the output power of the BMORs. However, the type of OLA TF chosen has a significant impact on the BER performance of the cascade. Lastly the analysis finds the linear approximation used in [6] to be a good TF approximation but the piecewise TF is a more realistic and realisable approximation than the linear TF.

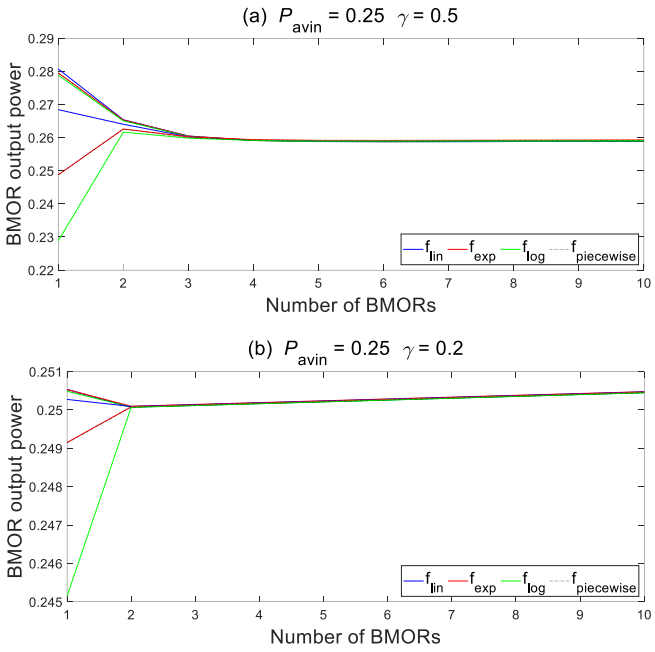

Fig. 11. Output power evaluation of each BMOR in the cascade for different OLA TFs with (a) $P_{\text{avin}} = 0.25$ and $\gamma = 0.5$, (b) $P_{\text{avin}} = 0.25$ and $\gamma = 0.2$ with $m_1 = m_2 = m_3 = m_4 = m_5 = m = 0.02, 0.14$ in each case.

REFERENCES

[1] O. Leclerc *et al.*, "Optical regeneration at 40 Gb/s and beyond," *J. Light. Technol.*, vol. 21, no. 11, pp. 2779–2790, Nov. 2003, doi: 10.1109/JLT.2003.819148.

[2] P. G. Patki *et al.*, "Recent Progress on Optical Regeneration of Wavelength-Division-Multiplexed Data," *IEEE J. Sel. Top. Quantum Electron.*, vol. 27, no. 2, pp. 1–12, 2021, doi: 10.1109/JSTQE.2020.3025482.

[3] A. E. Willner, S. Khaleghi, M. R. Chitgarha, and O. F. Yilmaz, "All-Optical Signal Processing," *J. Light. Technol.*, vol. 32, no. 4, pp. 660–680, 2014, doi: 10.1109/JLT.2013.2287219.

[4] D. Kulal, K. Pai, R. Padiyar, and P. D. Kakade, "Significance of 2R Continuous Mode Optical Regenerators (CMORs) in Optical Network Impaired by Optical Linear Crosstalk," 2019, doi: 10.1109/DISCOVER47552.2019.9008100.

[5] J. P. Jue, W.-. Yang, Y.-. Kim, and Q. Zhang, "Optical packet and burst switched networks: a review," *IET Commun.*, vol. 3, no. 3, pp. 334–352, Mar. 2009, doi: 10.1049/iet-com:20070606.

[6] P. N. Desai, A. J. Phillips, and S. Sujecki, "Modeling of burst mode 2R optical regenerator cascades for long-haul optical networks," *J. Opt. Commun. Netw.*, vol. 4, no. 4, 2012, doi: 10.1364/JOCN.4.000304.

[7] P. N. Desai, A. J. Phillips, and S. Sujecki, "Performance evaluation for 2R burst mode optical regenerator cascades in presence of co-channel phase uncorrelated crosstalk," 2012, doi: 10.1109/ICTON.2012.6254385.

[8] R. Sato, T. Ito, Y. Shibata, A. Ohki, and Y. Akatsu, "40-gb/s burst-mode optical 2R regenerator," *IEEE Photonics Technol. Lett.*, vol. 17, no. 10, pp. 2194–2196, Oct. 2005, doi: 10.1109/LPT.2005.856364.

[9] G. T. Kanellos *et al.*, "All-Optical 3R Burst-Mode Reception at 40 Gb/s Using Four Integrated MZI Switches," *J. Light. Technol.*, vol. 25, no. 1, pp. 184–192, Jan. 2007, doi: 10.1109/JLT.2006.888169.

[10] P. Zakynthinos *et al.*, "Cascaded Operation of a 2R Burst-Mode Regenerator for Optical Burst Switching Network Transmission," *IEEE Photonics Technol. Lett.*, vol. 19, no. 22, pp. 1834–1836, Nov. 2007, doi: 10.1109/LPT.2007.907580.

[11] D. Petrantonakis, P. Zakynthinos, D. Apostolopoulos, A. Poustie, G. Maxwell, and H. Avramopoulos, "All-Optical Four-Wavelength Burst Mode Regeneration Using Integrated Quad SOA-MZI Arrays," *IEEE Photonics Technol. Lett.*, vol. 20, no. 23, pp. 1953–1955, Dec. 2008, doi:

10.1109/LPT.2008.2005736.

[12] S.-K. Liaw and S. Chi, "Experimental investigation of a fiber Bragg grating integrated optical limiting amplifier with high dynamic range," *Opt. Eng.*, vol. 37, no. 7, pp. 2101–2103, 1998, doi: 10.1117/1.601800.

[13] H. Wessing, B. Sorensen, B. Lavigne, E. Balmefrezol, and O. Leclerc, "Combining control electronics with SOA to equalize packet- to-packet power variations for optical 3R regeneration in optical networks at 10 Gbit/s," in *Optical Fiber Communication Conference, 2004. OFC 2004*, 2004, vol. 1, p. 621.

[14] M. Presi, S. Gupta, N. Calabretta, G. Contestabile, and E. Ciaramella, "DPSK Packet-Level Power Equalization by means of Nonlinear Polarization Rotation in an SOA," in *2007 Photonics in Switching*, 2007, pp. 157–158, doi: 10.1109/PS.2007.4300792.

[15] S. V Pato, R. Meleiro, D. Fonseca, P. Andre, P. Monteiro, and H. Silva, "All-Optical Burst-Mode Power Equalizer Based on Cascaded SOAs for 10-Gb/s EPONs," *IEEE Photonics Technol. Lett.*, vol. 20, no. 24, pp. 2078–2080, 2008, doi: 10.1109/LPT.2008.2006629.

[16] N. Pleros, G. T. Kanellos, C. Bintjas, A. Hatziefremidis, and H. Avramopoulos, "Optical power limiter using a saturated SOA-based interferometric switch," *IEEE Photonics Technol. Lett.*, vol. 16, no. 10, pp. 2350–2352, 2004, doi: 10.1109/LPT.2004.833960.

[17] X. Wei, Y. Su, X. Liu, J. Leuthold, and S. Chandrasekhar, "10-Gb/s RZ-DPSK transmitter using a saturated SOA as a power booster and limiting amplifier," *IEEE Photonics Technol. Lett.*, vol. 16, no. 6, pp. 1582–1584, 2004, doi: 10.1109/LPT.2004.826732.

[18] B. Cao and J. E. Mitchell, "Modelling optical burst equalisation in next generation access network," in *2010 12th International Conference on Transparent Optical Networks*, 2010, pp. 1–4, doi: 10.1109/ICTON.2010.5549289.

[19] M. J. O'Mahony, C. Politi, D. Klonidis, R. Nejabati, and D. Simeonidou, "Future Optical Networks," *J. Light. Technol.*, vol. 24, no. 12, pp. 4684–4696, 2006, doi: 10.1109/JLT.2006.885765.

[20] Y. Su, X. Liu, and J. Leuthold, "Wide dynamic range 10-Gb/s DPSK packet receiver using optical-limiting amplifiers," *IEEE Photonics Technol. Lett.*, vol. 16, no. 1, pp. 296–298, 2004, doi: 10.1109/LPT.2003.818914.

[21] O. C. Graydon, M. N. Zervas, and R. I. Laming, "Erbium-doped-fiber optical limiting amplifiers," *J. Light. Technol.*, vol. 13, no. 5, pp. 732–739, May 1995, doi: 10.1109/50.387790.

[22] C. H. Kim, C. R. Giles, and Y. C. Chung, "Two-stage optical limiting fiber amplifier using a synchronized etalon filter," *IEEE Photonics Technol. Lett.*, vol. 10, no. 2, pp. 285–287, 1998, doi: 10.1109/68.655386.

[23] B. Charbonnier, N. E. Dahdah, and M. Joindot, "OSNR margin brought by nonlinear regenerators in optical communication links," *IEEE Photonics Technol. Lett.*, vol. 18, no. 3, pp. 475–477, Feb. 2006, doi: 10.1109/LPT.2005.863181.

[24] S. L. Tzeng, H. C. Chang, and Y. K. Chen, "Chirped-fibre-grating-based optical limiting amplifier for simultaneous dispersion compensation and limiting amplification in 10 Gbit/s G.652 fibre link," *Electron. Lett.*, vol. 35, no. 8, pp. 658–660, 1999, doi: 10.1049/el:19990435.

[25] Y.-K. Chen, S.-K. Liaw, W.-Y. Guo, and S. Chi, "Multiwavelength erbium-doped power limiting amplifier in all-optical self-healing ring network," *IEEE Photonics Technol. Lett.*, vol. 8, no. 6, pp. 842–844, 1996, doi: 10.1109/68.502113.

[26] M. J. Chawki, E. Delevaque, and L. Berthou, "WDM bidirectional optical power limiting amplifier including circulators, EDFA and fiber grating reflectors," in *Proceedings of European Conference on Optical Communication*, 1996, vol. 2, pp. 285–288 vol.2.

[27] Y. Su, L. Wang, A. Agarwal, and P. Kumar, "All-optical limiter using gain flattened fibre parametric amplifier," *Electron. Lett.*, vol. 36, no. 13, pp. 1103–1105, 2000, doi: 10.1049/el:20000798.

[28] M. Holtmannspoetter and B. Schmauss, "All Optical Limiter Based on Self Phase Modulation and Dispersive Chirping," in *2007 European Conference on Lasers and Electro-Optics and the International Quantum Electronics Conference*, 2007, p. 1, doi: 10.1109/CLEOE-IQEC.2007.4386110.

[29] M. R. G. Leiria and A. V. T. Cartaxo, "Impact of the Signal and Nonlinearity Extinction Ratios on the Design of Nonideal 2R All-Optical Regenerators," *J. Light. Technol.*, vol. 26, no. 2, pp. 276–285, Jan. 2008, doi: 10.1109/JLT.2007.909856.

[30] S. Primak, V. Kontorovich, and V. Lyandres, *Stochastic Methods and their Applications to Communications: Stochastic Differential Equations Approach*. 2005.